In a typical procedure,[6] 0.1 g of $[Fe(phen)_3](ClO_4)_3$ was dissolved in 50 mL of rigorously dried acetonitrile. Exactly 2.0 mL of this stock solution was placed in a quartz cuvette, which was then sealed with an air-tight septum. Initial UV absorbances (HP 8452 diode array spectrophotometer) were obtained for Fe(III) (586 nm, ϵ = 500) and background Fe(II) (510 nm, ϵ = 10 300) (due to trace water). The sample was then cooled to the appropriate temperature by using a recirculating cooling bath, and 10–20 μL of diene was added by syringe (1,4-dimethoxy-1,4-cyclohexadiene, a solid, was added from a stock solution in acetonitrile). Absorption spectra for Fe(III) and Fe(II) were measured automatically as a function of time. Oxidation of the diene to the arene was confirmed by quantitative GC analysis. Second-order rate constants for oxidation of a series of dienes are shown in Table I. In a corollary series of experiments, the effect of base, pyridine, on the rate of oxidation of 1,4-cyclohexadiene by $Fe(phen)_3^{3+}$ was measured,[7] and it was shown[5a] that electron transfer was rate determining for the overall process. (In typical experiments, no base other than the solvent was present.[8]) Oxidation of 1-methyl-1,4-cyclohexadiene (1-Me-1,4-CHD) by Fe(III) complexes of varying reduction potential[4] was effected, second-order rate constants were measured (Table II), and the correlation obtained between $\ln k_2$ and $E_{1/2}$ was excellent (Figure 1).

Although half-wave oxidation potentials have not been measured for all of the 1,4-dienes studied[9,10] (Table I), the general trend of increasing rate constant with increasing π-donor ability of the substituent group on a single double bond is obvious. Most significant is the observed 10^4 increase in k_2 for 4 vs 3, effected by replacement of hydrogen on the "unactivated" double bond of 1-MeO-1,4-CHD (3) by another donor methoxy group. This large rate enhancement, of the same magnitude as that observed for 1,4-CHD vs its 1,3-isomer,[10] strongly suggests a π interaction between the double bonds of the 1,4-diene in the rate-determining step for the oxidation reaction.[11] (Were the effect of placement of this second substituent merely inductive in nature, an *opposite*, and likely smaller, difference in rates would have been noted.) If not in the isolated molecule, at least in the presence of the Fe(III) oxidant, "homoconjugation" exists for this constrained system. Models for metalloenzyme-catalyzed oxidation of formally nonconjugated substrates must, therefore, consider outer-sphere oxidation to be a viable possibility when conformational mobility exists, which, by enabling "homoconjugative" interactions, lowers the oxidation potential of the conformer below that of its individual components.

Supplementary Material Available: General reaction scheme, UV spectrophotometric data for oxidation of the 1,4-diene to the arene, and data enabling calculation of rate constants for oxidation of the dienes (9 pages). Ordering information is given on any current masthead page.

(6) For example, Fe(III), 1.34 × 10⁻³ M; 1,4-cyclohexadiene, 0.177 M; k_{obsd} = 9.94 × 10⁻⁵ s⁻¹; k_2 = 5.62 × 10⁻⁴ s⁻¹ M⁻¹; average of four runs, k_2 = 5.2 (±1.0) × 10⁻⁴ s⁻¹ M⁻¹.

(7) For the complete reaction scheme, see supplementary material Figure 1, for which rate constants are given in supplementary material Table 3.

(8) For the use of acetonitrile solvent as a base in an electrochemical oxidation (of an arene), see: (a) Bewick, A.; Edwards, G. J.; Mellor, J. M.; Pons, B. S. *J. Chem. Soc., Perkin Trans. 2* 1977, *2*, 1952. (b) Bewick, A.; Mellor, J. M.; Pons, B. S. *Electrochim. Acta* 1980, *25*, 931. Interestingly, electrochemical oxidation of 1,4-cyclohexadiene in methanol or acetic acid yields only benzene, and no trapping products are observed.[9] Thus, apparently, a base even as weak as acetic acid can deprotonate the intermediate cation radical of 1,4-cyclohexadiene oxidation, and a nucleophile as good as methanol cannot intercept it.

(9) The oxidation potentials of a series of double bond substituted norbornadienes correlate with σ_p^+. See: Shono, T.; Ikeda, A.; Hayaishi, J.; Hakozaki, S. *J. Am. Chem. Soc.* 1975, *97*, 4261.

(10) Baltes, H.; Stork, L.; Schafer, H. J. *Chem. Ber.* 1979, *112*, 807.

(11) A similar transannular interaction has been proposed,[9] based on electrochemically measured oxidation potentials for several nonconjugated dienes.

Detection of Nuclear Overhauser Effects between Degenerate Amide Proton Resonances by Heteronuclear Three-Dimensional Nuclear Magnetic Resonance Spectroscopy

Mitsuhiko Ikura, Ad Bax,* G. Marius Clore,* and Angela M. Gronenborn

*Laboratory of Chemical Physics, Building 2
National Institute of Diabetes and Digestive and
Kidney Diseases
National Institutes of Health, Bethesda, Maryland 20892*

Received July 10, 1990

The key to protein structure determination by NMR lies in the identification of as many ^1H–^1H nuclear Overhauser effects (NOEs[1]) as possible in order to obtain a large set of approximate interproton distance restraints.[2] With the advent of a range of heteronuclear three-dimensional (3D) NMR experiments,[3–6] it has now become possible to obtain complete ^1H, ^{15}N, and ^{13}C assignments and to determine the 3D structures of proteins in the 15–25-kDa molecular weight range.[6,7] Despite these advances, it has remained impossible to observe NOEs between protons with degenerate chemical shifts. Such interactions occur repeatedly, both among aliphatic or aromatic protons and between sequential amide protons in helical proteins. Here we describe a 3D heteronuclear experiment that allows the observation of these NOEs and demonstrate its applicability for calmodulin, a protein of 148 residues and molecular weight 16.7 kDa.

Provided that the chemical shifts of the directly bonded heteronuclei are not degenerate, NOEs between degenerate protons can be detected in a 3D spectrum in which the heteronuclear chemical shifts are labeled in the F_1 and F_2 dimensions and the ^1H chemical shift is labeled in the F_3 dimension. In the case of NOEs involving NH protons, a ^1H–^{15}N HMQC–(^1H–^1H NOESY mixing)–^1H–^{15}N HMQC 3D experiment yields the necessary information. The pulse scheme is shown in Figure 1. This type of experiment is related to the triple-resonance $^{13}C/^{15}N$-edited 4D NOESY experiment[8] which permits observation of NOEs between degenerate ^{15}N and ^{13}C attached protons. Briefly, in the new 3D experiment heteronuclear multiple quantum coherence[9] is generated during the t_1 period, which is subsequently converted back into transverse ^1H magnetization. Thus, at the end of the t_1 period, ^1H magnetization is modulated by the shift of its attached ^{15}N nucleus. During the subsequent NOESY mixing period, τ_m, ^1H magnetization is transferred to its immediate spatial

(1) Abbreviations used: NOE, nuclear Overhauser effect; 3D, three-dimensional; HMQC, heteronuclear multiple quantum coherence; NOESY, nuclear Overhauser enhancement spectroscopy.

(2) (a) Wüthrich, K. *NMR of Proteins and Nucleic Acids*; Wiley, New York, 1986. (b) Clore, G. M.; Gronenborn, A. M. *CRC Crit. Rev. Biochem. Mol. Biol.* 1989, *24*, 479.

(3) (a) Fesik, S. W.; Zuiderweg, E. R. P. *J. Magn. Reson.* 1988, *78*, 588. (b) Marion, D.; Kay, L. E.; Sparks, S. W.; Torchia, D. A.; Bax, A. *J. Am. Chem. Soc.* 1989, *111*, 1515. (c) Marion, D.; Driscoll, P. C.; Kay, L. E.; Wingfield, P. T.; Bax, A.; Gronenborn, A. M.; Clore, G. M. *Biochemistry* 1989, *29*, 6150. (d) Messerle, B. A.; Wider, G.; Otting, G.; Weber, C.; Wüthrich, K. *J. Magn. Reson.* 1989, *85*, 608.

(4) (a) Kay, L. E.; Ikura, M.; Bax, A. *J. Am. Chem. Soc.* 1990, *112*, 888. (b) Fesik, S. W.; Eaton, H. L.; Olejniczak, E. T.; Zuiderweg, E. R. P.; McIntosh, L. P.; Dahlquist, F. W. *J. Am. Chem. Soc.* 1990, *112*, 886. (c) Bax, A.; Clore, G. M.; Driscoll, P. C.; Gronenborn, A. M.; Ikura, M.; Kay, L. E. *J. Magn. Reson.* 1990, *87*, 620. (d) Bax, A.; Clore, G. M.; Gronenborn, A. M. *J. Magn. Reson.* 1990, *88*, 425.

(5) Ikura, M.; Kay, L. E.; Bax, A. *Biochemistry* 1990, *29*, 4659.

(6) (a) Fesik, S. W.; Zuiderweg, E. R. P. *Q. Rev. Biophys.* 1990, *23*, 97. (b) Clore, G. M.; Gronenborn, A. M. *Annu. Rev. Biophys. Biophys. Chem.*, in press.

(7) (a) Driscoll, P. C.; Clore, G. M.; Marion, D.; Wingfield, P. T.; Gronenborn, A. M. *Biochemistry* 1990, *29*, 3542. (b) Driscoll, P. C.; Gronenborn, A. M.; Wingfield, P. T.; Clore, G. M. *Biochemistry* 1990, *29*, 4668. (c) Clore, G. M.; Bax, A.; Wingfield, P. T.; Gronenborn, A. M. *Biochemistry* 1990, *29*, 5671. (d) Clore, G. M.; Bax, A.; Driscoll, P. C.; Wingfield, P. T.; Gronenborn, A. M. *Biochemistry* 1990, *29*, 8172. (e) Clore, G. M.; Driscoll, P. C.; Wingfield, P. T.; Gronenborn, A. M. *J. Mol. Biol.* 1990, *214*, 811.

(8) Kay, L. E.; Clore, G. M.; Bax, A.; Gronenborn, A. M. *Science* 1990, *249*, 411.

(9) (a) Mueller, L. *J. Am. Chem. Soc.* 1979, *101*, 4481. (b) Bax, A.; Griffey, R. H.; Hawkins, B. L. *J. Magn. Reson.* 1983, *55*, 301.

Communications to the Editor

J. Am. Chem. Soc., Vol. 112, No. 24, 1990 9021
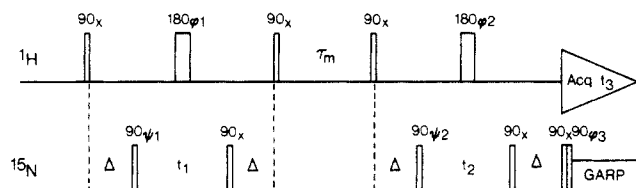
Figure 1. Pulse scheme for the 3D ^{1}H–^{15}N HMQC-(^{1}H–^{1}H NOE-SY)–^{1}H–^{15}N HMQC experiment. Phase cycling is as follows: $\psi 1 = x$, $-x$; $\psi 2 = 2(x)$, $2(-x)$; $\phi 1 = 4(x)$, $4(y)$, $4(-x)$, $4(-y)$; $\phi 2 = 8(x)$, $8(y)$, $8(-x)$, $8(-y)$; receiver $= (x,-x,-x,x)$, $2(-x,x,x,-x)$, $(x,-x,-x,x)$; $\phi 3 = x, -x$; receiver $= (x,-x,-x,x)$, $2(-x,x,x,-x)$, $(x,-x,-x,x)$. The TPPI-States method[11] is used to obtain quadrature in F_1 and F_2: after the entire 32-step phase cycle is completed, $\psi 1$ and $\psi 2$ are incremented independently by 90° for every t_1 and t_2 value, respectively, and data for $\psi 1 = x, y$ and $\psi 2 = x, y$ are stored separately and processed as complex data. In addition, every time t_1 is incremented, the receiver phase and $\psi 1$ are also incremented by 180°, and similarly every time t_2 is incremented, the receiver phase and $\psi 2$ are incremented by 180°. Decoupling during acquisition is achieved by using coherent ^{15}N GARP modulation.[21] The $90°_x$–$90°_{\pm x}$ ^{15}N pulse pair immediately prior to the start of GARP decoupling serves to reduce the intensity of modulation sidebands.[4c]

neighbors. At the end of τ_m, NH magnetization is converted back into heteronuclear multiple quantum coherence during t_2, before being detected during the acquisition period t_3. The same pulse sequence can be used to detect NOEs between aliphatic or aromatic protons with degenerate chemical shifts by replacing the ^{15}N pulses with ^{13}C pulses.

Figure 2 illustrates several slices taken from the ^{1}H–^{15}N HMQC-(NOESY)–HMQC 3D spectrum of uniformly ^{15}N labeled calmodulin (1.5 mM) in 95% H_2O/5% D_2O, 100 mM KCl, 6 mM Ca^{2+}, pH 6.3, at 35 °C. Figure 2a shows a section of an (F_1,F_3) slice taken perpendicular to the F_2 axis, demonstrating NOE interactions involving amide protons attached to nitrogens at 120.5 ppm, and protons for which the attached ^{15}N shift equals the F_1 coordinate. Of the large number of NOE interactions, that between Lys-77 and Met-76 (at $F_3 = 7.8$ ppm) is of particular interest. These residues are located near the middle of the so-called "central helix" of calmodulin, a long solvent-exposed helix observed in the crystal structure[10] which connects the two domains and which has been the subject of considerable interest. The NOE between Met-76 and Lys-75 is not visible in Figure 2a because the ^{15}N shifts of these two residues are degenerate. Their NOE interaction, however, is observed in the complementary 3D ^{1}H–^{15}N NOESY–HMQC spectrum[3] (unpublished).

Parts b and c of Figure 2 show sections of slices taken perpendicular to the F_3 axis. In these slices, the F_1 and F_2 coordinates are those of the ^{15}N atoms bonded to the originating and destination protons, respectively. In the case of NH protons with different chemical shifts, the NOE cross peaks appear in only one-half of the spectrum in a given (F_1,F_2) slice. Thus, in the case of an NOE interaction between amide protons A and B, one NOE cross peak appears in the slice with $F_3 = \delta A$, where δA is the proton shift of A, and the other one in the slice taken at $F_3 = \delta B$. In the case of NOEs involving NH protons with the same chemical shifts, on the other hand, cross peaks occur symmetrically about the diagonal in the same (F_1,F_2) slice.

The interaction between the two degenerate amide protons of Met-76 and Lys-77 is shown in Figure 2b, suggesting that these residues are part of a helical structure. Figure 2c illustrates the NOE interaction between another pair of degenerate NH protons, Met-144 and Met-145, with additional NOE cross peaks between Met-145 and Thr-146 and between Thr-143 and Met-144.

In calmodulin there are 12 pairs of sequential amide protons that differ by less than 0.05 ppm in chemical shift at 35 °C and
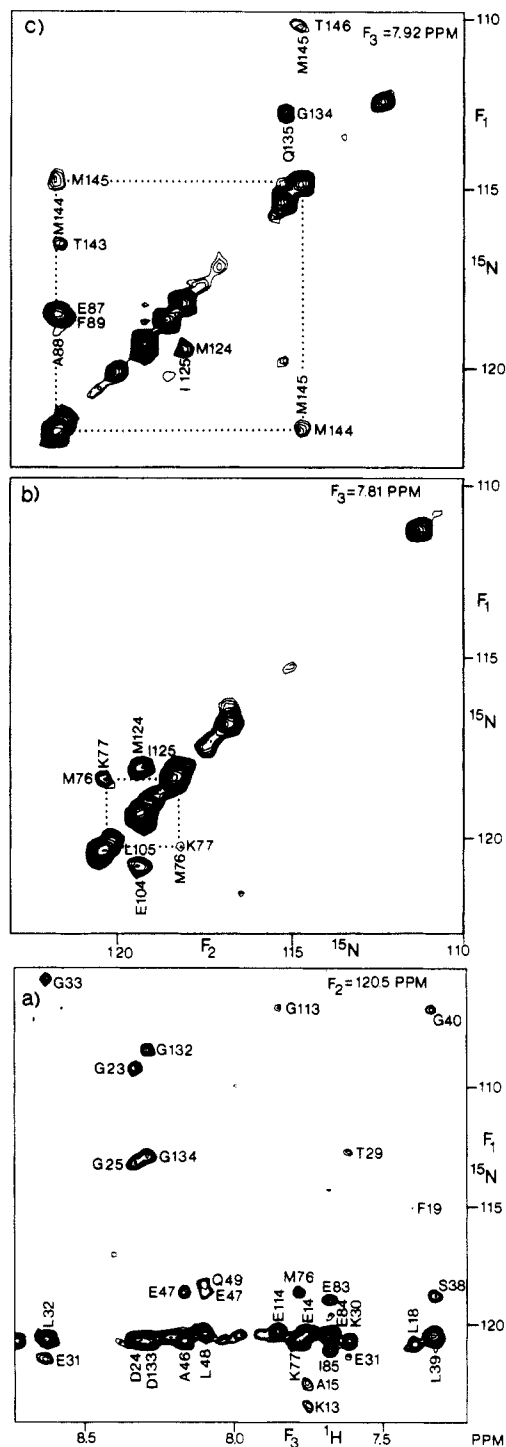

Figure 2. One selected ^{15}N(F_1)–^{1}H(F_3) slice (a) and two selected ^{15}N-(F_1)–^{15}N(F_2) slices at different ^{1}H(F_3) chemical shifts (b and c) of the ^{1}H–^{15}N HMQC-(^{1}H–^{1}H NOESY)–^{1}H–^{15}N HMQC 3D spectrum of 1.5 mM ^{15}N-labeled calmodulin recorded on a Bruker AM600 spectrometer. The delay Δ was set to 4.5 ms, and the NOE mixing time τ_m to 140 ms. The ^{1}H and ^{15}N carriers were positioned at 4.67 and 116.5 ppm, respectively. The water resonance was suppressed by coherent presaturation during the 1-s relaxation delay as well as during the NOESY mixing time τ_m. The acquired 3D data matrix comprised 64 complex $(t_1) \times 32$ complex $(t_2) \times 1024$ real (t_3) data points, and the total measuring time was ~91 h. The spectral width in F_1 and F_2 was 1666 Hz and in F_3 8064 Hz, with corresponding acquisition times of 38.4, 19.2, and 63.5 ms. The t_2 data was extended to 64 complex points by using linear prediction, and in addition, zero-filling was employed in all dimensions. The absorptive part of the final processed data matrix comprised $256 \times 128 \times 1024$ points with a digital resolution of 6.5, 13.0, and 7.88 Hz in F_1, F_2, and F_3, respectively. The spectrum was processed on a Sun Sparc Workstation using simple in-house routines[13] for the Fourier transform and linear prediction in F_2, together with the commercially available software package NMR2 (New Methods Research, Inc., Syracuse, NY) for processing the F_1–F_3 planes.

(10) (a) Babu, Y. S.; Sack, J. S.; Greenhough, T. J.; Bugg, C. E.; Means, A. R.; Cook, W. J. *Nature* **1985**, *315*, 37. (b) Kretsinger, R. H.; Ruderick, S. E.; Weissman, L. J. *J. Inorg. Biochem.* **1986**, *29*, 289.

(11) Marion, D.; Ikura, M.; Tschudin, R.; Bax, A. *J. Magn. Reson.* **1989**, *85*, 393.

(12) Shaka, A. J.; Barker, P. B.; Freeman, R. *J. Magn. Reson.* **1985**, *64*, 547.

(13) Kay, L. E.; Marion, D.; Bax, A. *J. Magn. Reson.* **1989**, *85*, 393.

pH 6.3, and for which NOEs could not be observed previously. These are as follows: Lys-30 and Glu-31 at the end of the first calcium binding loop; Met-36 and Arg-37 in helix 2; Gly-40 and Gln-41 in the turn following helix 2; Leu-48 and Gln-49 in helix 3; Met-76 and Lys-77 in helix 4; Asp-80 and Ser-81 and Val-91 and Phe-92 in helix 5; Leu-105 and Arg-106, His-107 and Val-108, and Leu-112 and Gly-113 in helix 6; Val-121 and Asp-122 in helix 7; and Met-144 and Met-145 in helix 8. Of these pairs, the interaction between the NH protons of His-107 and Val-108 could not be determined because both ^{15}N shifts are also degenerate, and no NOE was observed between Asp-80 and Ser-81. (Note that the latter may be due to the fast amide exchange rates of both Asp-80 and Ser-81.) For the remaining 10 pairs, clear NOE interactions were observed. In addition, there are eight pairs of protons with chemical shift differences between 0.05 and 0.10 ppm for which NOEs are observed much more clearly than in the corresponding 3D NOESY–HMQC spectrum.

The 3D experiment described here provides important additional data with regard to determining the 3D structure of proteins. The method is applicable for ^{15}N- or ^{13}C-enriched proteins and furnishes information that is complementary to the popular heteronuclear edited NOESY 3D experiment.[3] If overlap occurs in the 3D NOESY–HMQC spectrum, this will generally be resolved in the 3D HMQC–(NOESY)–HMQC spectrum, and vice versa.

Acknowledgment. We thank Lewis Kay and Guang Zhu for the development of the linear prediction software used in this work and Marie Krinks for preparation of the calmodulin sample. This research was supported by the AIDS Directed Anti-Viral Program of the Office of the Director of the National Institutes of Health (A.B., G.M.C., and A.M.G.).

An Unusual Oxidative Cyclization. A Synthesis and Absolute Stereochemical Assignment of (−)-Rocaglamide

Barry M. Trost,* Paul D. Greenspan, Bingwei V. Yang, and Mark G. Saulnier

Department of Chemistry, Stanford University Stanford, California 94305-5080

Rocaglamide (1), a novel natural product isolated from *Aglaia elliptifolia* Merr, has shown significant activity against P388 lymphocytic leukemia in CDF mice and human epidermoid carcinoma cells of the nasopharynx (in vitro).[1] While X-ray crystallography established the relative stereochemistry, the absolute stereochemistry remained to be defined.[1b] Furthermore, the high density of functionality makes the molecule a significant synthetic challenge.[2] Scheme I outlines our retrosynthetic analysis. In this paper, we record the first synthesis of rocaglamide, assignment of its absolute stereochemistry, and the development of a novel oxidative cyclization to create the dihydrobenzofuran ring (cf. 3 → 2).

Pd-catalyzed cycloaddition of the substituted TMM precursor 5 and acceptor 6 (R = CH₃) [5 mol % Pd(OAc)₂, 30 mol % (iC₃H₇O)₃P, PhCH₃, reflux][3,4] gave the cycloadduct 4⁵ (X = CH₂, R = CH₃, E/Z mixture) in 92% yield. Ozonolysis [2:1 CH₃OH/CH₂Cl₂, 78%; (CH₃)₂S] was accompanied by equilibration to the E isomer 4 (X = O, R = CH₃) in 77–79% yield.

The complex BF₃·CH₃OH (2 × 1.14 equiv) catalyzes (CH₂Cl₂, room temperature to reflux) the direct condensation of dimethyl phloroglucinol with the cyclopentanone 4 (X = O, R = CH₃) to give the adduct 3⁵ as a 2:1 mixture of olefin regioisomers (60% yield).

The oxidative cyclization of the regioisomeric olefin mixture 3 was envisioned to proceed via the allyl cation 7. Charge neutralization at the center of highest positive charge should provide the required regioselectivity. Attack of the oxygen on the least hindered face of 7 anti to the phenyl group should provide the necessary diastereoselectivity (i.e., 8), especially in an early-transition-state reaction. After much experimentation, DDQ⁶
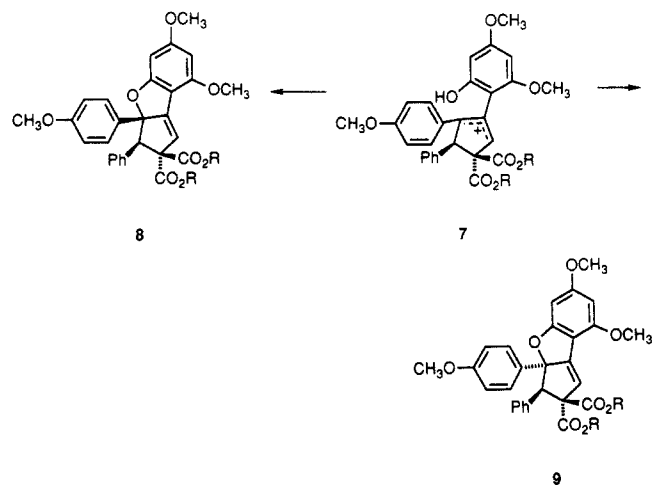
(THF, reflux) was found to give a 72–77% yield of a single crystalline cyclized product. Spectroscopic data clearly established the regiochemistry as predicted. Surprisingly, the stereochemistry proved to be that represented in 9⁵ (attack from the more hindered face!) as established by X-ray crystallography. Apparently the unusual compactness of the highly substituted molecule makes the developing aryl–aryl interaction dominate, a most unusual result, considering that the reaction should follow an early transition state.

Thus, an asymmetric synthesis of rocaglamide via our route must take into account an ultimate inversion of the stereochemistry of the phenyl group. Since the absolute stereochemistry was not known, we chose to embark upon a synthesis of the enantiomer depicted in formula 1. Cycloaddition of the oxazepinedione 10⁷ as described above (85% yield) followed by hydrolysis (NaOH, C₂H₅OH, reflux), esterification (CH₂N₂, C₂H₅OAc, room temperature), and ozonolysis (vide supra) gave the optically pure adduct 11,⁵ [α]_D = +27.8° (c = 2.1, CHCl₃). Condensation with

a) R = CH₃
b) R = CH₂Ph

(1) (a) McPhail, A. T.; King, M. L.; Chiang, C. C.; Ling, H. C.; Fujita, E.; Ochiai, M. *J. Chem. Soc., Chem. Commun.* **1982**, 1150. King, M. L.; Ling, C. H.; Wang, C. B.; Leu, S. C. *Med. Sci.* **1975**, *1*, 11. (b) Private communication from Professor McPhail.

(2) For earlier synthetic efforts, see: (a) Taylor, R. J. K.; Davey, A. E. *J. Chem. Soc., Chem. Commun.* **1987**, 25. (b) Kraus, G. A.; Sy, J. O. *J. Org. Chem.* **1989**, *54*, 77.

(3) For a review, see: Trost, B. M. *Angew. Chem., Int. Ed. Engl.* **1986**, *25*, 1.

(4) Cf.: Trost, B. M.; Renaut, P. *J. Am. Chem. Soc.* **1982**, *104*, 6668.

(5) This compound has been characterized spectroscopically and its elemental composition established by combustion analysis and/or high-resolution mass spectroscopy.

(6) Cf.: Gardilla, G.; Cricehio, R.; Merlini, L. *Tetrahedron Lett.* **1969**, 907.

(7) Trost, B. M.; Yang, B.; Miller, M. L. *J. Am. Chem. Soc.* **1989**, *111*, 6482.